Progress In Electromagnetics Research, PIER 76, 127–139, 2007

A DESIGNED MODEL ABOUT AMPLIFICATION AND COMPRESSION OF PICOSECOND PULSE USING CASCADED SOA AND NOLM DEVICE

J.-W. Wu

College of Mathematics & Physics
Hohai University
Nanjing 210098, P. R. China

D.-X. Tian

College of Physics & Information Technology
Chongqing Normal University
Chongqing 400047, P. R. China

H.-B. Bao

College of Mathematics & Physics
Hohai University
Nanjing 210098, P. R. China

Abstract—A novel technique for the amplification and the compression of an optical pulse is proposed. Based on cascaded a semiconductor optical amplifier (SOA) and a nonlinear optical loop mirror (NOLM), the chirping effect induced by the SOA and the cross phase modulation effect between the signal pulse and control pulse can be utilized to shape the pulse. The picosecond pulse amplification and compression are demonstrated in this paper. A good theoretical model is designed with optimal parameters. Results show that the output signal pulse with high peak power, narrow pulse width, and low pedestal can be obtained using the designed model, which is suited for furture 640 Gbps optical communications.

1. INTRODUCTION

Considerable attention has recently been focused on semiconductor optical amplifier (SOA) and their potential used in the optical communication system [1, 2]. The SOA has been generally considered suited for linear amplification compared to erbium doped fiber amplifier (EDFA) [3]. The SOA has generated more and more interest as a functional device in the area of long-haul optical transmission demonstrated by the results reported in references [4–6] recently. In this paper, we are also looking for the application of SOA and nonlinear optical loop mirror (NOLM) in high speed optical communications.

A number of intensity noise suppression techniques have been proposed to overcome these limitations and increase the system capacity [7–9]. One such a approach uses the nonlinear gain compression of a saturated SOA to suppress the intensity noise of the input thermal light [10]. This technique has the added benefit, in which ideally the SOA can also be used for signal modulation and amplification [11].

Due to high capability and long distance optical fiber communications developing quickly, the optical pulse of high peak power and narrow width is required. Because the optical pulse with low peak power and broad width is commonly generated using pulse source. So the technology of pulse amplification and compression must be applied in optical fiber communications field. We note that NOLM has been widely used for pulse compression and pulse pedestal suppression, but NOLM does not provide amplification because it is a passive device [12–14]. To obtain high quality pulse amplification and compression, one technique was used applying the erbium-doped nonlinear amplifying fiber loop mirror [15].

In this work, we design a novel model, which is a device of cascaded SOA and NOLM, for amplification and compression of picosecond optical pulse. How to enhance the pulse signal symmetry of 640 Gbps is emphasized in SOA transmission for fiber communications. However, the SOA may broaden and distort the 640 Gbps optical signal. Pump beam and control beam are both analyzed by solving the rate equations. The paper is organized as follows. The theoretical model and analysis are described in Section 2. The simulation results and discussions are presented in Section 3. We state a brief conclusion in Section 4.

2. DESIGNED MODEL & THEORY

Figure 1 shows the configuration of pulse amplification and compression based on an SOA and an NOLM. After a signal optical pulse is amplified by the SOA, it goes through an isolator and is split into the clockwise and counterclockwise signal pulses at the coupler. The control optical pulse couples into the NOLM at one wavelength division multiplexer (WDM), and propagates along the fiber loop clockwise. After the pulse propagates a round, the control pulse is outputted at WDM2, and the clockwise and counterclockwise signal pulses collide and interfere in time domain, so the high quality signal pulse can be obtained.

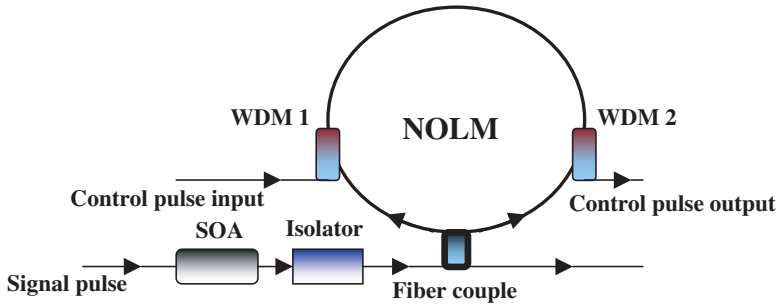

Figure 1. Design model of pulse amplification and compression based on SOA and NOLM.

In order to understand the carrier-induced nonlinearity in the semiconductor optical amplifier, a theoretical model is developed in this section. Assuming that the reflectivity of facets of the SOA is equal to zero, the SOA has been segmented into a number of smaller sections. The theoretical analysis can be used for looking for the numerical solutions of the differential carrier rate equation for each section. The propagation equations of a control pulse and a signal pulse can be represented as follows [16, 17]. In the different location of SOA, the carrier density N, optical power P and phase ϕ can be described as [16–19]

$$\frac{\partial N_j}{\partial T} = \frac{I}{qV} - \frac{N_j}{\tau_c} - \frac{\Gamma g_i(N_j)}{\hbar\omega A_{cross}}\bar{P}_j \tag{1}$$

$$\frac{\partial P_j}{\partial Z} = (\Gamma g(N_j) - \alpha_{\text{int}})P_j \tag{2}$$

$$\frac{\partial \phi_j}{\partial Z} = -\frac{1}{2}\Gamma\alpha_j g(N_j) \tag{3}$$

where j is the jth segment, N_j, P_j and ϕ_j are the carrier density, optical power and phase in the jth segment, respectively, $T(= t - Z/V_g$, V_g is the group velocity, Z is a different location) is the normal time, I is the injection current, V is the active volume, q is the electron charge, τ_c is the carrier lifetime, $1/\tau_c = A + BN + CN^2$, A, B and C are the nonradioactive, bimolecular and Auger recombination constant, respectively, Γ is the confinement factor, $\hbar\omega$ is the photon energy, A_{cross} is the cross section mode, α_{int} is the internal loss, $\bar{P_j}$ and α_j are the average optical power and linewidth enhanced factor in the jth segment, respectively, and can be described by [20]

$$\begin{aligned} \bar{P_j} &= \frac{1}{\Delta L}\int_0^{\Delta L} P_{j-1} e^{((\Gamma g(N_j)-\alpha_{\text{int}})z)} dZ \\ &= \frac{(e^{((\Gamma g(N_j)-\alpha_{\text{int}})\Delta L)}-1)}{(\Gamma g(N_j)-\alpha_{\text{int}})\Delta L} P_{j-1} \end{aligned} \tag{4}$$

$$\alpha_j = -\frac{4\pi}{\lambda_s}\left[\frac{dn}{dN}\Big/\frac{dg}{dN}\right] \tag{5}$$

where dn/dN is the index with the carrier density variation, dg/dN is the gain with the carrier density variation, λ_s is the wavelength of the signal pulse, ΔL is the length of each section, P_{j-1} is the output power of the $(j-1)$th section, $g(N_j)$ is the gain described by [21]

$$g(N_j) = a_1(N_j - N_0) - a_2(\lambda_s - \lambda_N)^2 + a_3(\lambda_s - \lambda_N)^3 \tag{6}$$

where a_1 is the differential gain coefficient, N_0 is the carrier density required for transparency, a_2 and a_3 are the width of gain spectrum and the experience constant of gain asymmetry, λ_N is the wavelength of the gain peak related to the carrier density described by [20]

$$\lambda_N = \lambda_0 - a_4(N_j - N_0) \tag{7}$$

where λ_0 is the wavelength of the gain peak for transparency, a_4 is the experience constant with the wavelength of the gain peak variation with the carrier density.

Let the input signal pulse and the control pulse be a free chirp Gaussian pulse and a Lorentzian pulse, respectively. They can be described by

$$P_s = P_{s0}\exp\left(-\frac{T^2}{T_0^2}\right) \tag{8}$$

$$P_c = P_{c0}\left[1 + \left(\frac{2T}{T_0}\right)^2\right]^{-1} \tag{9}$$

where P_{s0} and P_{c0} are the peak power of the input signal and control pulse, respectively, T_0 is the half width at $1/e$ intensity point.

Equations (1) to (8) can be solved numerically, and the envelop of the output signal pulse can be written as

$$A_s = \sqrt{P_{SOA}} \exp(i\phi_{SOA}) \tag{10}$$

where P_{SOA} and Φ_{SOA} are the power and phase of the output signal.

Under neglecting the loss of the coupler, isolator, wave division multiplexed and NOLM, the propagation equations of the signal and control pulse in an NOLM can be described by [22–26]

$$\frac{\partial A_s^+}{\partial Z} + \frac{i}{2}\beta_{2s}\frac{\partial^2 A_s^+}{\partial T^2} = i\gamma_s[|A_s^+|^2 + 2|A_c|^2]A_s^+ \tag{11}$$

$$-\frac{\partial A_s^-}{\partial Z} + \frac{i}{2}\beta_{2s}\frac{\partial^2 A_s^-}{\partial T^2} = i\gamma_s|A_s^-|^2 A_s^- \tag{12}$$

$$\frac{\partial A_c}{\partial Z} + d\frac{\partial A_c}{\partial T} + \frac{i}{2}\beta_{2c}\frac{\partial^2 A_c}{\partial T^2} = i\gamma_c\left[|A_c|^2 + 2\left|A_s^+\right|^2\right]A_c \tag{13}$$

The initial conductions can be described by

$$A_s^+(0,T) = (1-K)^{1/2}A_s(T) \tag{14}$$

$$A_s^-(0,T) = iK^{1/2}A_s(T) \tag{15}$$

where A_s^+, A_s^-, and A_c are the clockwise, counterclockwise signal pulse envelope, and control pulse envelop in the NOLM, respectively, $d(= 1/V_{gc} - 1/V_{gs})$ is the group velocity detuning between A_c and A_s^+, $\beta_{2i}(i = s, c)$ is the group velocity dispersion, $\gamma = n_2\omega_0/cA_{eff}$ is the nonlinear coefficient, n_2 is the nonlinear refractive index, A_{eff} is the cross section area of the optical fiber, ω_0 is the control frequency of the optical pulse, c is the light velocity of the vacuum, K is the coupler power splitting ratio, since the pulse width is shorter than the propagation time in the NOLM, the cross phase modulation is neglected for counterpropagation pulses, and the cross phase is only included for copropagation pulses.

After $A_s^+(0,0)$ and $A_s^-(0,0)$ propagate for a circle in the NOLM, their interference occurs at the fiber coupler, so the output envelop can be described by [19]

$$A_{out}(L,T) = (1-K)^{\frac{1}{2}}A_s^+(L,T) + iK^{\frac{1}{2}}A_s^-(L,T) \tag{16}$$

In the end, the output signal pulse forms, peak gain, width compression factor, and pedestal energy can be researched. The pulse

peak gain, width compression factor, and pedestal energy can be written as

$$G(dB) = 10\log(\frac{P_{sout}}{P_{s0}}) \tag{17}$$

$$Compression\ Factor = \frac{T_{\sin}}{T_{sout}} \tag{18}$$

$$Pedestal\ energy\ (\%) = \frac{|E_{total} - E_{gauss}|}{E_{total}} \times 100\% \tag{19}$$

where P_{s0} and P_{sout} are the peak power of the input signal and output signal pulse, respectively, T_{sin} and T_{sout} are the full width at the half maximum of the input signal and output signal pulses, respectively, E_{total} is the total energy of the outputted signal pulse, E_{gauss} is the total energy of a Gaussian pulse having the same peak power and width (at $1/e$ intensity point) as those of the outputted signal pulse. To investigate the dynamics evolution of pulse, Equations (1)–(3) and (11)–(13) can be solved numerically by using finite-difference time-domain (FDTD) method [27–29].

3. RESULTS & DISCUSSIONS

Figure 2 shows the peak power gain, compression factor, and corresponding pedestal energy of the output signal pulse as a function of the time delay. Because of the gain saturation effect of the SOA, the amplified optical pulse is asymmetric, thus the initial time delay is defined as the time difference between the peak power of the input signal and the peak power of the input control pulse in NOLM, a negative time delay means that the signal pulse is ahead of the control pulse and a positive time delay means that the signal pulse lags behind the control pulse. The data used for calculations and all parameters of the SOA are shown in Table 1.

From Figure 2 we can see that the variation in time delay (T_d) has an obvious impact on tuning the peak gain, the compression factor, and the pedestal energy. The peak gain and the compression factor first experience increasing and then decreasing with the variation of T_d. The peak gain and the compression factor reach the maximum while T_d is near 5 ps. When the $T_d = 5$ ps, the pedestal energy has the least value. These performances can be explained: after the Gaussian signal pulse is amplified, the chirp of the amplified signal pulse by the SOA increases almost linearly over the central part of the pulse [21]. Such a linear chirp implies that the pulse can be compressed in a dispersion medium such as an optical fiber if it experiences anomalous group velocity

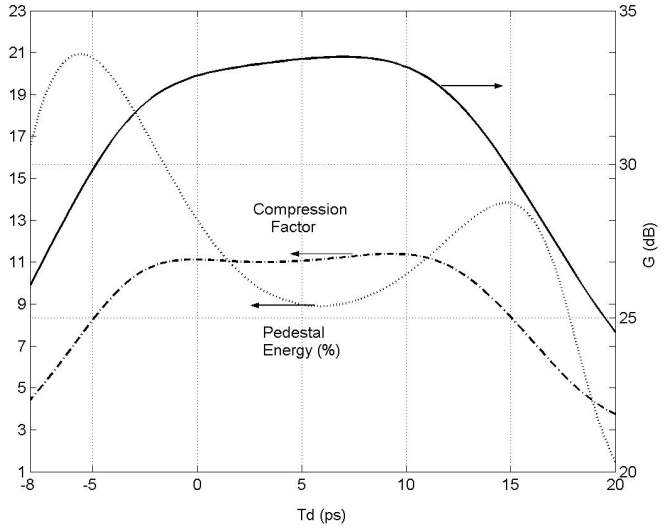

Figure 2. Variation curves of the peak gain and compression factor of an output signal pulse are against T_d.

dispersion during its propagation in that medium. The peak power can be increased and the location of peak power is also downshifted. However, the cross phase modulation occurred between the clockwise signal pulse and the control pulse, then a quantity of opposite chirp is generated by the cross phase modulation in the central part of signal pulse. So under the chirp of the SOA and the cross phase modulation, the signal pulse can be compressed deeply, and the peak power can also be increased. The quantity of the nonlinear phase can be obtained by the signal pulse through the cross phase modulation so that there is a different nonlinear phase between the clockwise signal pulse and counterclockwise signal pulse. Owing to the transmission function of the NOLM, the counterpropagation signal pulses should interfere in the coupler. When T_d is near 5 ps, the overlapped part of the signal pulse and control pulse is the largest. So the effect of the cross phase modulation is enhanced deeply, and the chirp and nonlinear phase of signal pulse has a large value. The output signal pulse coming from the NOLM has the properties of high peak power gain, high compression factor, and little pedestal energy. Figure 3 shows the corresponding pulse shapes. From Figure 2 and Figure 3, we can find that the high quality signal pulse can be obtained with tuning $T_d \approx 5$ ps.

Figure 4 shows the variation curves of the peak gain, compression

Table 1. Parameters for calculation of the pulse variation in SOA.

Symbol	Definition	Value
P_{c0}	Peak power of controlling pulse	100 mW
P_{s0}	Peak power of signal pulse	1 mW
T_0	Width of signal optical pulse	20 ps
λ_c	Second order super-Gaussian controlling pulse	1550 nm
λ_s	Gaussian signal pulse	1545 nm
L	Length of each section	2380 m
A_{cross}	Cross-sectional area of the active layer	0.3 um^2
V	Volume of each SOA	150 um^3
I	Injection current	150 mA
N_0	Carrier density at transparency	$0.9 \times 10^{24}/\text{m}^3$
λ_0	Peak wavelength at transparency	1605 nm
α_{int}	Internal loss	20 cm^{-1}
Γ	Confinement factor	0.3
A	Recombination coefficient	$2.5 \times 10^8\ \text{s}^{-1}$
B	Recombination coefficient	$1.0 \times 10^{-16}\ \text{m}^3/\text{s}$
C	Recombination coefficient	$0.94{\times}10^{-40}\ \text{m}^6/\text{s}$
a_1	Gain factor	$2.5 \times 10^{-20}\ \text{m}^2$
a_2	Gain factor	$7.4 \times 10^{18}\ \text{m}^{-3}$
a_3	Gain factor	$3.155{\times}10^{25}\ \text{m}^{-4}$
a_4	Gain factor	$3 \times 10^{-32}\ m^4$
q	Electron charge	1.6×10^{-19} C
d	Group velocity	8 fs
A_{eff}	Cross section area of optical fiber	50e−12 m^2
c	Light velocity of vacuum	3×10^8 m/s
K	Coupler power splitting ratio	0.5
n_2	Nonlinear reference index	$3.2 \times 10^{-20}\ \text{m}^2/\text{W}$
β_{2i}	Group velocity dispersion	$-20\ \text{ps}^2/\text{Km}$

factor, and pedestal energy against the variation of the control pulse with initial peak power. Using the time delay parameter of $T_d = 8.7$ ps, others are identical to those used in Figure 2. From Figure 4 we can see that the signal pulse peak gain and compression factor are first increased, and then decreased with the variation of P_{c0}, and the peak

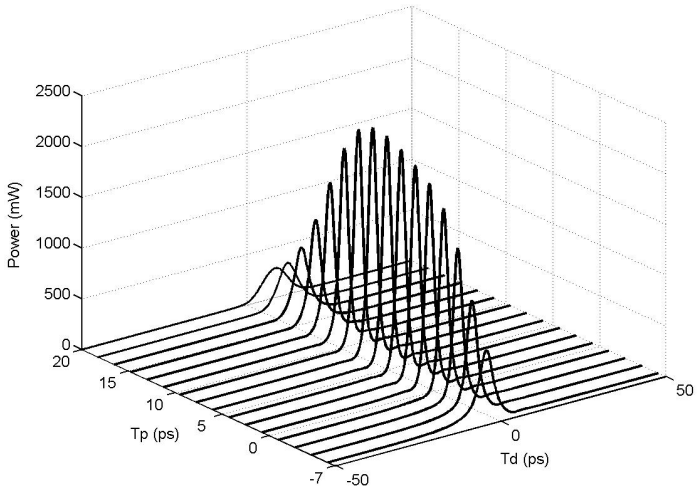

Figure 3. Shape forms of an output signal pulse are against T_d.

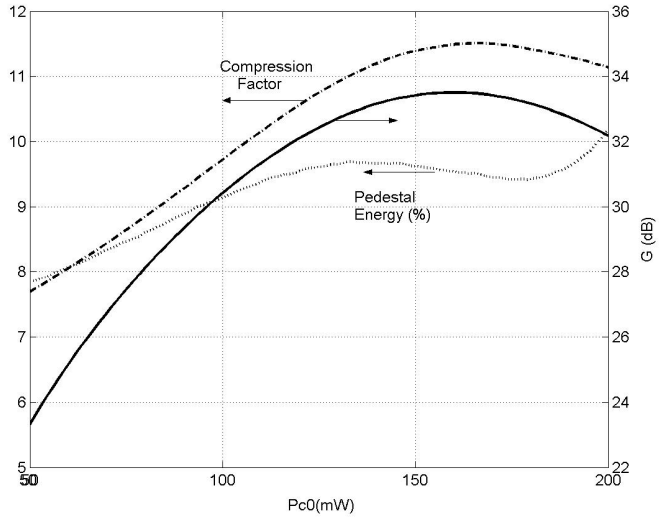

Figure 4. Variation curves of the peak gain and compression factor of an output signal pulse are against P_{c0}.

gain and compression factor have a maximum near $P_{c0} \approx 150\,\mathrm{mW}$. The pedestal energy remains below 10% over a variation range of $50\,\mathrm{mW} \sim 200\,\mathrm{mW}$. The reason is that the effect of the cross phase modulation is little with small P_{c0}, so the peak gain and compression factor are small. But as P_{c0} is increased, the effect of the cross phase modulation is enhanced between the signal pulse and control pulse, and the peak gain and compression factor can be increased gradually. Figure 5 shows the corresponding pulse shapes as a function of the control pulse peak power.

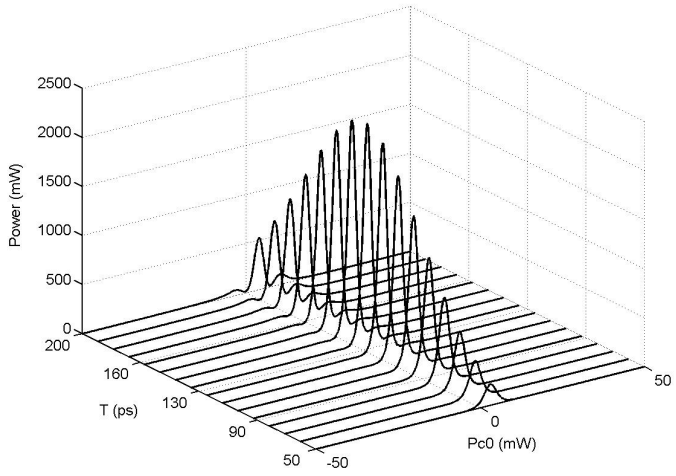

Figure 5. Shape forms of an output signal pulse are against P_{c0}.

4. CONCLUSION

In this paper, we have proposed a novel model for amplification and compression of an optical pulse with cascaded SOA and NOLM. The novel technique demonstrates that the amplification and compression of the optical pulse can be enhanced by adjusting the system parameters. The work is helpful for high speed optical communications and signal processions.

REFERENCES

1. O'Mahony, M. J., "Semiconductor laser amplifiers for use in future fiber systems," *J. Lightwave Technol.*, Vol. 6, No. 4, 4531–544, 1988.

2. Olsson, N. A., "Lightwave systems with optical amplifiers," *J. Lightwave Technol.*, Vol. 7, No. 7, 1071–1092, 1989.
3. Stubkjaer, K. E., et al., "Wavelength conversion devices and techniques," *Proc. 22nd Eur. Conf. Optical Communication*, 4.33–4.40, Oslo, Norway, Sept. 1996.
4. Jennen, J. G. L., R. C. J. Smets, H. de Waardt, G. N. van den Hoven, and A. J. Boot, "4×10 Gbit/s NRZ transmission in the 1310 nm window over 80 km of standard signal mode fiber using semiconductor optical amplifiers," *Proc. 24th Eur. Conf. Optical Communication*, Madrid, Spain, 235–236, 1998.
5. Boscolo, S., S. K. Thritsyn, R. Bhamber, V. K. Mezentsev, and S. V. Grigoryan, "Feasibility of soliton-like DPSK transmission at 40 Gb/s with in-line semiconductor optical amplifier," *IEEE Photo. Technol. Lett.*, Vol. 18, No. 3, 490–492, 2006.
6. Ciaramella, E., A. D'Errico, R. Proietti, and G. Contestabile, "WDM-POLSK transmission systems by using semiconductor optical amplifiers," *J. Lightwave Technol.*, Vol. 24, No. 11, 4039–4046, 2006.
7. Keating, A. J. and D. D. Sampson, "Reduction of excess intensity noise in spectrum-sliced incoherentlight for WDM applications," *J. Lightwave Technol.*, Vol. 15, No. 1, 53–61, 1997.
8. Han, J. H., J. W. Ko, J. S. Lee, and S. Y. Shin, "0.1-nm narrow bandwidth transmission of a 2.5 Gb/s spectrum-sliced incoherent light channel using an all-optical bandwidth expansion technique at the receiver," *IEEE Photon. Technol. Lett.*, Vol. 10, No. 10, 1501–1503, 1998.
9. Koyama, F., T. Yamatoya, and K. Iga, "Highly gain-saturated GaInAsP/InP SOA modulator for incoherent spectrum-sliced light source," *Conf. Indium Phosphide and Related Materials*, 439–442, 2000.
10. Zhao, M., G. Morthier, and R. Baets, "Analysis and optimization of intensity noise reduction in spectrum-sliced WDM systems using a saturated semiconductor optical amplifier," *IEEE Photon. Technol. Lett.*, Vol. 14, No. 3, 390–392, 2002.
11. Healey, P., P. Townsend, C. Ford, L. Johnston, P. Townley, I. Lealman, L. Rivers, S. Perrin, and R. Moore, "Spectral slicing WDM-PON using wavelength-seeded reflective SOAs," *Electron. Lett.*, Vol. 37, No. 19, 1181–1182, 2001.
12. Phillips, I. D., P. N. Kean, N. J. Doran, I. Bennion, D. A. Pattison, and A. D. Ellis, "Simultaneous clock recovery and data regeneration using a nonlinearoptical loop mirror as an all-optical mixer," *Optical Fiber Communication Conf.*, 273–274, 1997.

13. Lee, J. H., T. Kogure, and D. J. Richardson, "Wavelength tunable 10-GHz 3-ps pulse source using a dispersion decreasing fiber-based nonlinear optical loop mirror," *IEEE J. Selected Topics in Quantum Electron.*, Vol. 10, No. 1, 181–185, 2004.
14. Yu, J., A. Clausen, H. N. Poulsen, P. Jeppesen, X. Zheng, and C. Peucheret, "40 Gb/s wavelength conversion in a cascade of a SOA and a NOLM and demonstration of extinction ratio improvement," *Electron. Lett.*, Vol. 36, No. 11, 963–964, 2000.
15. Wai, P. K. A. and W. Cao, "Simultaneous amplification and compression of ultrashort fundamental solitons in an erbiumdoped nonlinear amplifying fiber loop mirror," *IEEE J. Quantum Electron.*, Vol. 39, No. 4, 555–561, 2003.
16. Willner, A. E. and W. Shieh, "Optical spectral and power parameters for all-optical wavelength shifting single stage, fanout, and cascadability," *J. Lightwave Technol.*, Vol. 13, No. 5, 771–781, 1995.
17. Yu, J. and P. Jeppesen, "Improvement of cascaded semiconductor optical amplifier gates by using holding light injection," *J. Lightwave Technol.*, Vol. 19, No. 5, 614–623, 2001.
18. Mathlouthi, W., P. Lemieux, M. Salsi, A. Vannucci, A. Bononi, and L. A. Rusch, "Fast and efficient dynamic WDM semiconductor optical amplifier model," *J. Lightwave Technol.*, Vol. 24, No. 11, 4356–4365, 2006.
19. Matsumoto, A., K. Nishimura, K. Utaka, and M. Usami, "Operational design on high-speed semiconductor optical amplifier with assist light for application to wavelength converters using cross-phase modulation," *IEEE J. Quantum Electron.*, Vol. 42, No. 3, 313–323, 2006.
20. Ye, Y., X. Zheng, H. Zhang, Y. Li, and Y. Guo, "Theoretical study on wavelength conversion based on cross phase modulation using semiconductor optical amplifiers," *J. Infrared and Millmeter Waves*, Vol. 22, No. 12, 1785–1792, 2002.
21. Agrawal, G. P. and N. A. Olsson, "Self-phase modulation and spectral broadening of optical pulses in semiconductor laser amplifiers," *IEEE J. Quantum Electron.*, Vol. 25, No. 11, 2297–2306, 1989.
22. Agrawal, G. P., *Nonlinear Fiber Optics*, Academic, New York, 1995.
23. Biswas, A. and S. Konar, "Theory of dispersion-managed optical solitons," *Progress In Electromagnetics Research*, PIER 50, 83–134, 2005.

24. Shwetanshumala, A. Biswas, and S. Konar, "Dynamically stable super Gaussian solitons in semiconductor doped glass fibers," *J. of Electromagn. Waves and Appl.*, Vol. 20, No. 7, 901–912, 2006.
25. Crutcher, S., A. Biswas, M. D. Aggarwal, and M. E. Edwards, "Oscillatory behavior of spatial solitons in two-dimensional waveguides and stationary temporal power law solitons in optical fibers," *J. of Electromagn. Waves and Appl.*, Vol. 20, No. 6, 761–772, 2006.
26. Biswas, A., S. Konar, and E. Zerrad, "Soliton-soliton interaction with parabolic law nonlinearity," *J. of Electromagn. Waves and Appl.*, Vol. 20, No. 7, 927–939, 2006.
27. Kung, F. and H. T. Chuah, "A finite-difference time-domain (FDTD) software for simulation of printed circuit board (PCB) assembly," *Progress In Electromagnetics Research*, PIER 50, 299–335, 2005.
28. Gong, Z. Q. and G. Q. Zhu, "FDTD analysis of an anisotropically coated missile," *Progress In Electromagnetics Research*, PIER 64, 69–80, 2006.
29. Chen, X., D. Liang, and K. Huang, "Micro wave imaging 3-D buried objects using parallel genetic algorithm combined with FDTD technique," *J. of Electromagn. Waves and Appl.*, Vol. 20, No. 13, 1761–1774, 2006.